

Effects of Array Weight Errors on Parallel Interference Cancellation Receiver in Uplink Synchronous and Asynchronous DS-CDMA Systems

Yong-Seok Kim, Seung-Hoon Hwang, and Keum-Chan Whang

This paper investigates the impacts of array weight errors (AWE) in an antenna array (AA) on a parallel interference cancellation (PIC) receiver in uplink synchronous and asynchronous direct sequence code division multiple access (DS-CDMA) systems. The performance degradation due to an AWE, which is approximated by a Gaussian distributed random variable, is estimated as a function of the variance of the AWE. Theoretical analysis, confirmed by simulation, demonstrates the tradeoffs encountered between system parameters such as the number of antennas and the variance of the AWE in terms of the achievable average bit error rate and the user capacity. Numerical results show that the performance of the PIC with the AA in the DS-CDMA uplink is sensitive to the AWE. However, either a larger number of antennas or uplink synchronous transmissions have the potential of reducing the overall sensitivity, and thus improving its performance.

Keywords: Array weight error, antenna array, parallel interference cancellation, DS-CDMA, uplink synchronous transmission.

I. Introduction

Direct sequence code division multiple access (DS-CDMA) systems exhibit a user capacity limitation in the sense that there exist a maximum number of users that can simultaneously communicate over multipath fading channels for a specified level of performance per user. This limitation is caused by co-channel interference, which includes both multiple access interference (MAI) between the users and intersymbol interference imposed by the channel-induced dispersion. Therefore, the interference rejection techniques for combining a cell site adaptive antenna array (AA) and an interference cancellation (IC) have been proposed to combat the effects of the co-channel interference, and thus increase system capacity [1], [2]. When the AA is used to suppress interference arriving from different directions with the desired signal, IC is used to cancel interference signals originating from the same direction which are not suppressed in the AA.

Previous studies [3] have assumed ideal error-free array weights and have neglected the effects of array weight errors (AWE) on the performance of combined AA and IC receivers in DS-CDMA systems. However, it is important to know how these errors degrade performance, since the actual performance of the system is dependent upon the implemented weights which are directly used as an estimate of the array response vector to regenerate the signals in the IC receiver. Besides AWE, the effects of the array geometry error must not be ignored in the direction-finding algorithm for the AA weights. However, in this paper, a blind algorithm is considered without estimating the user's direction. Therefore, it is reasonable that the array

Manuscript received Dec. 16, 2003; revised July 18, 2004.

Yong-Seok Kim (phone: +82 2 2123 8504, email: dragon@commsys.yonsei.ac.kr) and Keum-Chan Whang (email: dragon@yonsei.ac.kr) are with the Department of Electrical and Electronic Engineering, Yonsei University, Seoul, Korea.

Seung-Hoon Hwang (email: shh03v@ecs.soton.ac.uk) is with the School of Electronics and Computer Science, University of Southampton, UK.

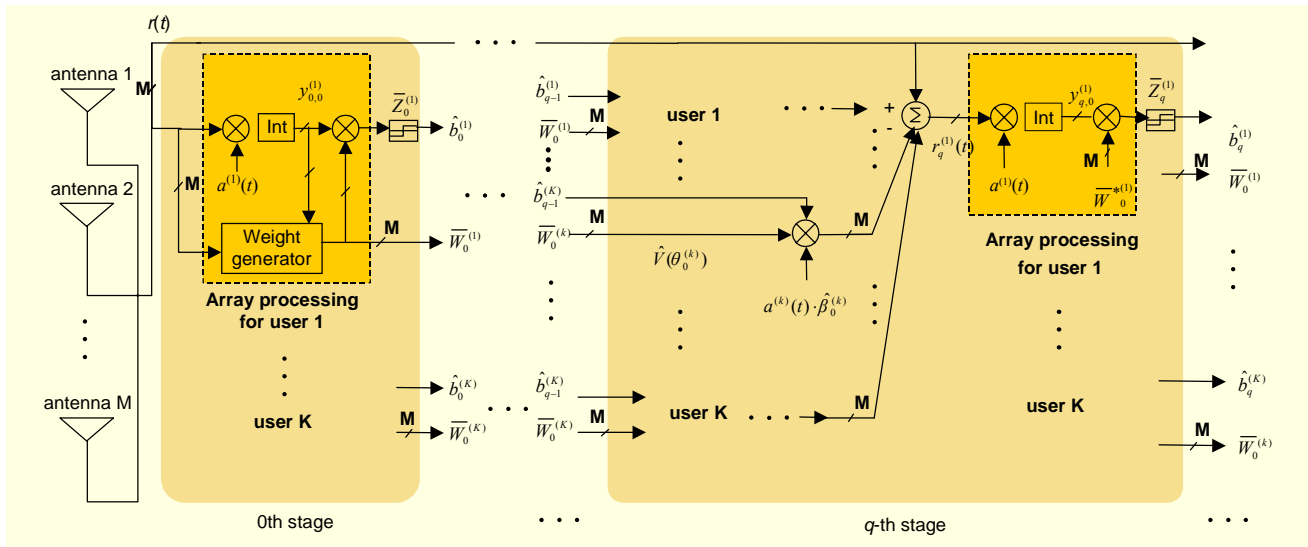


Fig. 1. Block diagram of a combined AA and PIC receiver structure.

geometry error be considered as one of the factors resulting in the AWE. The AWE which arises due to imperfect knowledge concerning the array element positions, computational error caused by finite-precision arithmetic, quantization error, and implementation error caused by component variation [4], is to be modeled by a Gaussian distributed random variable [5]. Therefore, this work investigates the effects of AWE on the performance of the combined AA and parallel IC (PIC) receivers in the DS-CDMA uplink. The performance degradation due to the AWE, which is approximated by a Gaussian distributed random variable, is estimated as a function of the variance of the AWE. Theoretical analysis, confirmed by simulation, demonstrates the tradeoffs between the system parameters, such as the number of antennas and the variance of the AWE in terms of the achievable average bit error rate (BER), and the user capacity of two different uplink scenarios, namely that of a conventional asynchronous transmission and a synchronous transmission. Uplink synchronous transmission has been proposed for reducing the effects of MAI in terrestrial and broadband mobile systems [6]-[9] with the additional benefit of having a lower multi-user detection, or IC complexity [10], as well as showing an improved AA, or IC performance [11], [12] than that of equivalent asynchronous systems.

The remainder of the paper is organized as follows. The channel and system model are outlined in section II. The performance is analytically derived and evaluated for both uplink synchronous and asynchronous scenarios in section III. Our numerical results are presented in section IV, while our conclusions are provided in section V.

II. Channel and System Model

We consider DS-CDMA uplink in a single cell where the

cell site AA has the M elements. The received signals are assumed to undergo frequency-selective Rayleigh fading channels. Perfect power control is also assumed. Figure 1 shows the block diagram of a combined AA and PIC receiver structure. In this paper, the PIC is considered because the PIC structure has many advantages such as a relatively small processing time, fairness among users, and performance stability. Assuming the presence of K active users, the signal received at the input of the AA is expressed as

$$\mathbf{r}(t) = \sqrt{2P} \sum_{k=1}^K \sum_{l=0}^{L^{(k)}-1} \beta_l^{(k)} \mathbf{V}(\theta_l^{(k)}) b^{(k)}(t - \tau_l^{(k)}) \times a^{(k)}(t - \tau_l^{(k)}) \cos[\omega_c t + \psi_l^{(k)}] + \mathbf{n}(t), \quad (1)$$

where P is the average power, $a^{(k)}(t) = v^{(k)}(t)$ is a user specific pseudo-noise (PN) sequence for an asynchronous scenario, and $a^{(k)}(t) = v(t) \cdot g^{(k)}(t)$ is an orthogonal sequence multiplied by the PN sequence for a synchronous scenario, where $v(t) = \sum_{j=-\infty}^{\infty} v_j P_{T_c}(t - jT_c)$ is the PN randomization sequence which is common to all the uplink channels in a cell and used for maintaining the CDMA system's orthogonality and $g^{(k)}(t) = \sum_{j=-\infty}^{\infty} g_j^{(k)} P_{T_g}(t - jT_g)$ is the orthogonal channelization sequence [6]. Here, $P_{\tau}(t) = 1$ for $0 \leq t \leq \tau$, and $P_{\tau}(t) = 0$, otherwise. The durations of the chips in the PN and the orthogonal sequences are denoted by T_c and T_g , respectively, and we assume for simplicity that T_g is equal to T_c . The term $b^{(k)}(t)$ is the k -th user's baseband modulated data waveform, $\tau_l^{(k)}$ is the propagation delay, and $\psi_l^{(k)}$ is the carrier phase. The symbol $\beta_l^{(k)}$ is assumed to be an independent Rayleigh random variable showing a fading

magnitude of the k -th user on the l -th propagation path. Assuming that Rayleigh fading is encountered, the received signal magnitude $l = 0, 1, \dots, L^{(k)}-1$ has a probability density function given by

$$p(\beta_l^{(k)}) = \frac{2\beta_l^{(k)}}{\Omega_l^{(k)}} \exp\left(-\frac{(\beta_l^{(k)})^2}{\Omega_l^{(k)}}\right). \quad (2)$$

The parameter $\Omega_l^{(k)}$ is the second moment of $\beta_l^{(k)}$ (i.e. $\Omega_l^{(k)} = E[(\beta_l^{(k)})^2]$) with $\sum_{l=0}^{L^{(k)}-1} \Omega_l^{(k)} = 1$, and we assume that $\Omega_l^{(k)}$ is related to the second moment of the main tap $\Omega_0^{(k)}$ in the exponential multipath intensity profile (MIP) according to

$$\Omega_l^{(k)} = \Omega_0^{(k)} \exp(-l\delta), \quad \text{for } 0 \leq l \leq L^{(k)}-1, \quad \delta \geq 0, \quad (3)$$

where δ reflects the decay rate of the average path magnitude as a function of the path delay. Note that in a realistic channel model the main path typically conveys more than half of the total received signal power [13]-[15]. The vector $\mathbf{V}(\theta_l^{(k)})$ is the array response vector of M antennas for the k -th user's l -th path as expressed in [16]

$$\mathbf{V}(\theta_l^{(k)}) = [1 \quad \exp(-j2\pi d \cos\theta_l^{(k)} / \lambda) \quad \dots \quad \exp(-j2(M-1)\pi d \cos\theta_l^{(k)} / \lambda)]^T, \quad (4)$$

where the array geometry is determined as a uniform linear array of M identical sensors, d is the spacing between the sensors, and λ is the wavelength of the carrier frequency. All signals from MS arrive at AA in the cell site with the mean direction of arrival, $\theta_l^{(k)}$, which are uniformly distributed in $[0, \pi)$. Finally, $\mathbf{n}(t)$ is the spatially and temporally white Gaussian noise vector with a zero mean and per-antenna noise variance, which is stated as $E\{\mathbf{n}(t)\mathbf{n}^H(t)\} = \sigma_n^2 \mathbf{I}$, where \mathbf{I} is the $M \times M$ identity matrix, σ_n^2 is the antenna noise variance with $\eta_0/2$, and superscript H denotes the Hermitian-transpose operator.

A RAKE receiver using maximal ratio combining is considered, where the number of fingers, L_r , is a variable less than or equal to the number of resolvable propagation paths associated with the k -th user, $L^{(k)}$. Note that a correlator receiver is shown in Fig. 1 as a simple example. We assume for the sake of simplicity coherent binary phase shift keying data modulation. Perfect channel estimation is also assumed. Note that the array weight vector at the initial stage of the PIC is repeatedly used at every subsequent stage [2], [6]. The received signal for the reference user ($k=1$) at the output of the q -th stage in the IC is expressed as

$$\mathbf{r}_q^{(1)}(t) = \mathbf{r}(t) - \sum_{k=2}^K \sum_{l=0}^{L_r-1} \sqrt{2P} \hat{\beta}_l^{(k)} \hat{\mathbf{V}}(\theta_l^{(k)}) \hat{b}_{q-1}^{(k)}(t - \tau_l^{(k)}) \times a^{(k)}(t - \tau_l^{(k)}) \cos[\omega_c t + \psi_l^{(k)}], \quad (5)$$

where $\hat{\beta}_l^{(k)}$ is the estimate of the Rayleigh fading magnitude of the k -th user's l -th path, $\hat{b}_{q-1}^{(k)}$ denotes the tentative decision measured at the $(q-1)$ th stage in the PIC, and $\hat{\mathbf{V}}(\theta_l^{(k)})$ is the estimate of the array response vector of the k -th user's l -th path at the q -th stage of the PIC. In general, structures of [17], [18], $\hat{\mathbf{V}}(\theta_l^{(k)})$ is assumed to be equal to $\overline{\mathbf{W}}_l^{(k)}$, which is the array weight vector for the AA in the $(q-1)$ th stage of the PIC.

Assuming that the MAI is spatially white, the optimal array weight of the k -th user at the l -th path can be shown to be $\overline{\mathbf{W}}_l^{(k)} = \mathbf{V}(\theta_l^{(k)})$ [19]. This assumption does hold when the total number of paths is large and the code length used in CDMA systems is long. However, in practice, the estimated optimal weights are corrupted by random errors which arise due to imperfect knowledge of the array element positions and the direction of arrival of the desired signal [5], and thus the estimated weight is presented as $\overline{\mathbf{W}}_l^{(k)} = \mathbf{V}(\theta_l^{(k)}) + \boldsymbol{\varepsilon}_l^{(k)}$, where $\boldsymbol{\varepsilon}_l^{(k)}$ is the M -dimensional additive random noise vector component with $E[\boldsymbol{\varepsilon}_l^{(k)}] = 0$ and $E[\boldsymbol{\varepsilon}_l^{(k)} \boldsymbol{\varepsilon}_l^{(k)H}] = \sigma_\varepsilon^2 \cdot \mathbf{I}$, for all k and l . Here, σ_ε^2 represents the variance of the AWE with the same value for all active users and the multipath index [5].

The matched filter output for the reference user's l -th path becomes

$$\mathbf{y}_{q,l}^{(1)} = \int_{\tau_l^{(1)}}^{\tau_l^{(1)}+T} \mathbf{r}_q^{(1)}(t) \cdot a^{(1)}(t - \tau_l^{(1)}) \cos[\omega_c t + \psi_l^{(1)}] dt. \quad (6)$$

Applying the common criterion of maximizing the signal-to-interference-plus-noise ratio, we can determine the optimal array weights at the q -th stage in the PIC [19]. Additionally, using the general analysis of the PIC in [20], the output signal at the AA becomes

$$\bar{\mathbf{z}}_{q,l}^{(1)} = \overline{\mathbf{W}}_l^{(1)H} \cdot \mathbf{y}_{q,l}^{(1)} = \bar{S}_{q,l}^{(1)} + \bar{I}_{q,l,mai}^{(1)} + \bar{I}_{q,l,si}^{(1)} + \bar{I}_{q,l,ni}^{(1)}, \quad (7)$$

where

$$\bar{S}_{q,l}^{(1)} = \sqrt{\frac{P}{2}} \beta_l^{(1)} C_{ll}^{(1,1)} b_0^{(1)T} T, \quad (7a)$$

$$\begin{aligned} \bar{I}_{q,l,mai}^{(1)} = & \sqrt{\frac{P}{2}} \sum_{k=2}^K \sum_{j=0}^{L^{(k)}-1} \beta_j^{(k)} \cos[\psi_j^{(k)}] \\ & \times \left\{ \left[C_{lj}^{(1,k)} b_{-1}^{(k)} - \bar{C}_{lj}^{(1,k)} \hat{b}_{q-1,1}^{(k)} \right] R_{k1} [\tau_j^{(k)}] \right. \\ & \left. + \left[C_{lj}^{(1,k)} b_0^{(k)} - \bar{C}_{lj}^{(1,k)} \hat{b}_{q-1,0}^{(k)} \right] \hat{R}_{k1} [\tau_j^{(k)}] \right\}, \end{aligned} \quad (7b)$$

$$\bar{I}_{q,l,si}^{(1)} = \sqrt{\frac{P}{2}} \sum_{\substack{j=0 \\ j \neq l}}^{L^{(1)}-1} \beta_j^{(1)} C_{lj}^{(1,1)} \cos[\psi_{lj}^{(1)}] \\ \times \left\{ b_{-1}^{(1)} R_{l1}[\tau_{lj}^{(1)}] + b_0^{(1)} \hat{R}_{l1}[\tau_{lj}^{(1)}] \right\} \quad \text{and} \quad (7c)$$

$$\bar{I}_{q,l,ni}^{(1)} = \int_{\tau_l^{(1)}}^{\tau_l^{(1)}+T} \bar{\mathbf{W}}_l^{(1)H} \mathbf{n}(t) \beta_l^{(1)} a^{(1)}(t - \tau_l^{(1)}) \\ \times \cos[\omega_c t + \psi_l^{(1)}] dt, \quad (7d)$$

where $b_0^{(1)}$ is the information bit to be detected, $b_{-1}^{(1)}$ is the preceding bit, while $\tau_{lj}^{(k)} = \tau_j^{(k)} - \tau_l^{(1)}$ and $\psi_{lj}^{(k)} = \psi_j^{(k)} - \psi_l^{(1)}$. Here, $C_{lj}^{(1,k)} = \bar{\mathbf{W}}_l^{(1)H} \cdot \mathbf{V}(\theta_j^{(k)})$ represents the spatial correlation between the array weight vector of the 1st user's l -th path and the array response vector of the k -th user's j -th path in the q -th stage of the PIC, and $\bar{C}_{lj}^{(1,k)} = \bar{\mathbf{W}}_l^{(1)H} (\mathbf{V}(\theta_j^{(k)}) + \boldsymbol{\varepsilon}_l^{(k)}) = C_{lj}^{(1,k)} + \Delta_{lj}^{(1,k)}$ is also defined as the estimated spatial correlation between the array weight vector and the estimated array response vector where $\Delta_{lj}^{(1,k)}$ is the estimated error of spatial correlation. The PN or Walsh-PN continuous partial correlation functions, $R_{kl}(\tau) = \int_0^\tau a^{(k)}(t-\tau) \cdot a^{(l)}(t) dt$ and $\hat{R}_{kl}(\tau) = \int_\tau^T a^{(k)}(t-\tau) \cdot a^{(l)}(t) dt$, can be expressed by a discrete aperiodic cross-correlation function [6], [21]. From (7a) thru (7d), we see that the output consists of four terms. The first term represents the desired signal component to be detected. The second term represents the MAI inflicted by the $(K-1)$ other simultaneous users after being cancelled at the q -th stage in the PIC. The third term is the self-interference (SI) imposed by the reference user, while the fourth term represents the effects of the AWGN. From (7), we can obtain the RAKE output, $\bar{z}_q^{(1)} = \sum_{l=0}^{L_r-1} \beta_l^{(1)} \cdot \bar{z}_{q,l}^{(1)}$.

III. Analysis of the Effects of AWE on the Combined AA and PIC Receiver

1. Uplink Asynchronous Scenario

To analyze the performance of AA with the PIC receiver used for a conventional asynchronous DS-CDMA uplink, we employ the Gaussian assumption in the BER calculation, since it is common, and since it was found to be quite accurate even when used for small values of K (< 10), provided that the BER is 10^{-3} or higher [22]. The variance of MAI, conditioned on $\beta_l^{(1)}$, can be expressed as follows:

$$\sigma_{q,l,mai}^2 = \frac{E_b T (N-1)}{6N^2} \left\{ \beta_l^{(1)} \right\}^2 \\ \times \sum_{k=2}^K \sum_{j=0}^{L^{(k)}-1} \Omega_j^{(k)} \left\{ 4P_e^{(k)} (q-1) E \left[\left\{ C_{lj}^{(1,k)} \right\}^2 \right] + E \left[\left\{ \Delta_{lj}^{(1,k)} \right\}^2 \right] \right\}, \quad (8)$$

where E_b is the signal energy per bit, T is the data bit duration, and N is the processing gain. The term $P_e^{(k)}(q-1)$ is the BER at the $(q-1)$ th stage in the PIC. More detailed derivations of spatial correlation statistics such as $E[\{C_{lj}^{(1,k)}\}^2]$ and $E[\{\Delta_{lj}^{(1,k)}\}^2]$ are described in the Appendix. The conditional variance of $\sigma_{q,l,si}^2$ is approximated by

$$\sigma_{q,l,si}^2 \approx \frac{E_b T}{4N} \left\{ \beta_l^{(1)} \right\}^2 \sum_{\substack{j=0 \\ j \neq l}}^{L^{(1)}-1} \Omega_j^{(1)} E \left[\left\{ C_{lj}^{(1,1)} \right\}^2 \right], \quad (9)$$

while the variance of the AWGN noise term is given by

$$\sigma_{q,l,ni}^2 = \frac{T \eta_0 \left(E \left[\left\{ C_{ll}^{(1,1)} \right\}^2 \right] - (M^2 - M) \right)}{4} \left\{ \beta_l^{(1)} \right\}^2. \quad (10)$$

From (8) thru (10), the variance of total interference is equal to the sum of all interference and noise terms, $\sigma_{q,T}^2 = \sum_{l=0}^{L_r-1} (\sigma_{q,l,mai}^2 + \sigma_{q,l,si}^2 + \sigma_{q,l,ni}^2)$. Finally, the mean output of the receiver is

$$U_q = \sqrt{\frac{E_b T}{2}} \sum_{l=0}^{L_r-1} \left\{ \beta_l^{(1)} \right\}^2 E \left[C_{ll}^{(1,1)} \right]. \quad (11)$$

Therefore, the SNR at the output of the receiver may be written as

$$\gamma_s = \frac{U_q^2}{\sigma_{q,T}^2} = \left\{ \frac{(K-1)(N-1)q(L_r, \delta) \{4AP_e(q-1) + C\}}{3N^2} \right. \\ \left. + \frac{\{q(L_r, \delta) - 1\}A}{2N} + \frac{\eta_0 \{B - (M^2 - M)\}}{2E_b \Omega_0} \right\}^{-1} \\ \times \frac{M^2}{\Omega_0} \sum_{l=0}^{L_r-1} \left\{ \beta_l^{(1)} \right\}^2, \quad (12)$$

where

$$P_e^{(1)}(q-1) = \dots = P_e^{(K)}(q-1) = P_e(q-1),$$

$$\Omega_0^{(k)} = \Omega_0,$$

$$q(L_r, \delta) = \sum_{l=0}^{L_r-1} \exp(-l\delta),$$

$$A = M\sigma_\varepsilon^2 + \sum_{i=0}^{M-1} (i+1)J_0(2\pi di/\lambda)J_0(-2\pi di/\lambda) \\ + \sum_{i=M}^{2(M-1)} (2M-i-1)J_0(2\pi di/\lambda)J_0(-2\pi di/\lambda),$$

$$B = M\sigma_\varepsilon^2 + M^2, \text{ and}$$

$$C = M(\sigma_\varepsilon^2 + \sigma_\varepsilon^4)$$

as shown in the Appendix. Assuming the $\{\beta_n^{(l)}\}$ are an i.i.d. Rayleigh distribution with an exponential MIP, the probability density function of $X = \sum_{n=0}^{L_r-1} \{\beta_n^{(l)}\}^2$ is

$$p_X(x) = \sum_{k=0}^{L_r-1} \frac{\pi_k}{\Omega_k} \exp(-x/\Omega_k). \quad (13)$$

Therefore, the average BER can be expressed as

$$P_e = \int_0^\infty Q(\sqrt{\gamma_s}) \cdot \sum_{k=0}^{L_r-1} \frac{\pi_k}{\Omega_k} \exp(-x/\Omega_k) dx \\ = \frac{1}{2} \sum_{k=0}^{L_r-1} \pi_k \left[1 - \sqrt{\frac{\Omega_k \cdot \Xi}{2 + \Omega_k \cdot \Xi}} \right] \quad (14)$$

where

$$Q(x) = \frac{1}{\sqrt{2\pi}} \int_x^\infty \exp\left(-\frac{u^2}{2}\right) du,$$

$$\pi_k = \prod_{\substack{i=0 \\ i \neq k}}^{L_r-1} \frac{x_k - x_i}{x_k - x_i} = \prod_{\substack{i=0 \\ i \neq k}}^{L_r-1} \frac{\Omega_k}{\Omega_k - \Omega_i}, \text{ and}$$

$$\Xi = \left\{ \frac{(K-1)(N-1)q(L_r, \delta)\Omega_0 \{4AP_e(q-1) + C\}}{3N^2M^2} \right. \\ \left. + \frac{\{q(L_r, \delta) - 1\}\Omega_0 A}{2NM^2} + \frac{\eta_0 \{B - (M^2 - M)\}}{2E_b M^2} \right\}^{-1}.$$

2. Uplink Synchronous Scenario

In this subsection, an uplink synchronous scenario is considered.

The performance is analyzed to investigate the effect of AWE on the combined AA and PIC structure in the synchronous DS-CDMA uplink. In the synchronous DS-CDMA uplink, the MSs are differentiated by the orthogonal codes, and the timing alignment among mainpaths is achieved with the adaptive timing control in a similar manner to a closed loop power control algorithm [6], [8]. Here, the arrival time of the first RAKE receiver branch signal is assumed to be synchronous, while the remaining branch signals are asynchronous. Therefore, we can consider the arrival times of the paths are modeled as synchronous for the first RAKE receiver branch (i.e., $l=0$) but as asynchronous in the rest of the branches (i.e., $l \geq 1$). Extending the derivations of [7] and [11], the variance of the MAI for $l=0$, conditioned on $\beta_l^{(l)}$, can be expressed as follows:

$$\sigma_{q,0,mai}^2 = \frac{E_b T(2N-3)}{12N(N-1)} \{\beta_0^{(1)}\}^2 \\ \times \sum_{k=2}^K \sum_{j=1}^{L^{(k)}-1} \Omega_j^{(k)} \left\{ 4P_e^{(k)}(q-1)E\left[\{C_{0j}^{(1,k)}\}^2\right] + E\left[\{\Delta_{0j}^{(1,k)}\}^2\right] \right\}. \quad (15)$$

The variance of the MAI for $l \geq 1$ can be formulated as

$$\sigma_{q,l,mai}^2 = \frac{E_b T(N-1)}{6N^2} \{\beta_l^{(1)}\}^2 \\ \times \sum_{k=2}^K \sum_{j=0}^{L^{(k)}-1} \Omega_j^{(k)} \left\{ 4P_e^{(k)}(q-1)E\left[\{C_{lj}^{(1,k)}\}^2\right] + E\left[\{\Delta_{lj}^{(1,k)}\}^2\right] \right\}. \quad (16)$$

From (9) – (11), (15), (16), the SNR at the output of the receiver may be expressed as (17).

The average BER may be evaluated as

$$P_e = \int_0^\infty \int_0^\infty Q(\sqrt{\gamma_s}) \cdot \sum_{k=1}^{L_r-1} \frac{\pi'_k}{\Omega_k} \exp\left(-\frac{x}{\Omega_k}\right) \cdot \frac{1}{\Omega_0} \exp\left(-\frac{y}{\Omega_0}\right) dx dy, \quad (18)$$

$$\gamma_s = \frac{U_q^2}{\sigma_{q,T}^2} = \left\{ \frac{(K-1)(2N-3)\{q(L_r, \delta) - 1\}\{4AP_e(q-1) + C\}}{6N(N-1)} \cdot \frac{\{\beta_0^{(1)}\}^2}{\{\beta_0^{(1)}\}^2 + \sum_{l=1}^{L_r-1} \{\beta_l^{(1)}\}^2} \right. \\ \left. + \frac{(K-1)(N-1)q(L_r, \delta)\{4AP_e(q-1) + C\}}{3N^2} \cdot \frac{\sum_{l=1}^{L_r-1} \{\beta_l^{(1)}\}^2}{\{\beta_0^{(1)}\}^2 + \sum_{l=1}^{L_r-1} \{\beta_l^{(1)}\}^2} + \frac{\{q(L_r, \delta) - 1\}A}{2N} + \frac{\eta_0 \{B - M^2 + M\}}{2E_b \Omega_0} \right\}^{-1} \\ \times \frac{M^2}{\Omega_0} \sum_{l=0}^{L_r-1} \{\beta_l^{(1)}\}^2. \quad (17)$$

where

$$\pi'_k = \prod_{\substack{i=1 \\ i \neq k}}^{L_r-1} \frac{x_k}{x_k - x_i} = \prod_{\substack{i=1 \\ i \neq k}}^{L_r-1} \frac{\Omega_k}{\Omega_k - \Omega_i},$$

$$X = \sum_{n=1}^{L_r-1} \{\beta_n^{(1)}\}^2,$$

$$p_X(x) = \sum_{k=1}^{L_r-1} \frac{\pi'_k}{\Omega_k} \exp\left(-\frac{x}{\Omega_k}\right),$$

$$Y = \{\beta_0^{(1)}\}^2,$$

$$p_Y(y) = \frac{1}{\Omega_0} \exp\left(-\frac{y}{\Omega_0}\right) \text{ for } y \geq 0.$$

IV. Numerical Results

In this section, we investigate the effects of the various parameters on the achievable BER performance of the combined AA with a PIC receiver in the uplink asynchronous and synchronous DS-CDMA systems over a dispersive Rayleigh fading channel exhibiting an exponential MIP with the decay factor of $\delta = 1.0$. In all evaluations, the processing gain is assumed to be 128, the iteration number in the PIC is set to be zero (i.e., RAKE receiver) or one, and the number of propagation paths and RAKE receiver fingers is assumed to be the same for all users, namely two.

Figures 2, 3, and 4 show the effect of the AWE in the uplink conventional asynchronous DS-CDMA systems. Figure 2 shows the achievable average BER performance as a function of E_b/N_0 , when the variances of AWE are assumed to be 0.0 and 0.5. For illustration, $K=12$ and $M=4$ are assumed. Analytical results confirmed by simulation, demonstrate the effects of the

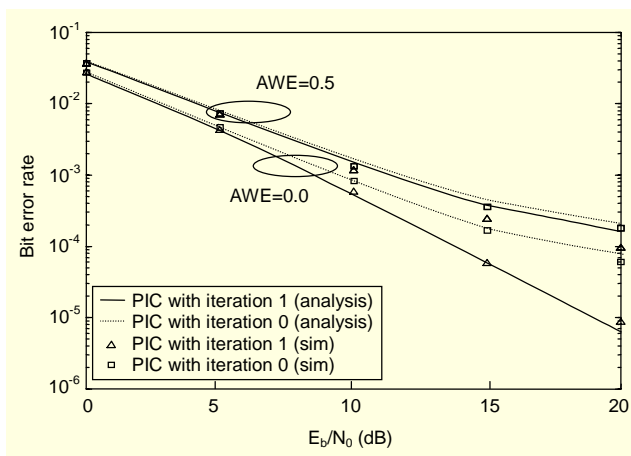


Fig. 2. BER vs. E_b/N_0 in asynchronous DS-CDMA uplink ($K=12$, $M=4$).

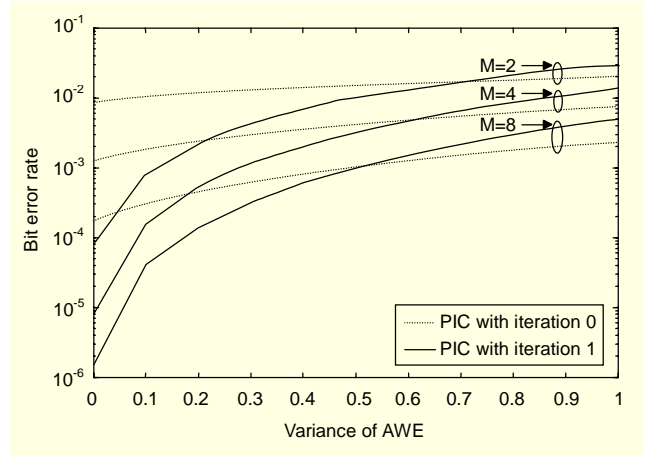


Fig. 3. BER vs. variance of the AWE in asynchronous DS-CDMA uplink ($K=72$, $E_b/N_0 = 20$ dB).

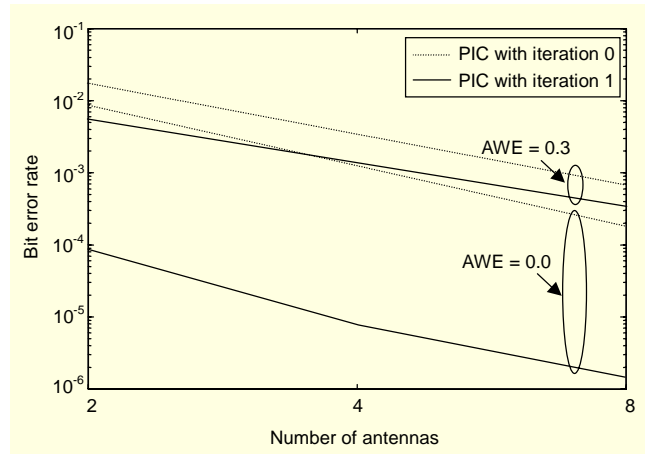


Fig. 4. BER vs. number of antenna in asynchronous DS-CDMA uplink ($K=72$, $E_b/N_0=20$ dB).

AWE on the PIC receiver. It is shown that 0.5 dB in terms of E_b/N_0 is more greatly required in the PIC receiver with one iteration at $\text{BER}=10^{-3}$. That is to say, the performance of the PIC receiver with one iteration is more sensitive to the AWE than that of the RAKE receiver only because the AWE may directly affect the performance of the PIC. Figure 3 shows the average BER performance comparisons between the PIC receiver with one iteration and the RAKE receiver structures as a function of the variance of the AWE for the various values of the number of antennas such as 2, 4, and 8, when $K=72$ and $E_b/N_0=20$ dB. Note that there is a cross point between the BER curves of the PIC receiver with one iteration and the RAKE receiver, when the variance of the AWE increases from 0 to 1. This indicates that the larger AWE may make the performance of the PIC receiver worse than that of the RAKE receiver, even though the PIC is employed to improve the performance of the RAKE-only receiver. Additionally, it is shown that the tolerable margin of the variance of the AWE may increase, as the

number of antennas increases. For example, the tolerable margin of the AWE is equal to 0.1 when $M=2$, while it increases to 0.6 when $M=8$ at the BER of 10^{-3} . This result demonstrates that a larger number of antennas can be a possible solution to improve the performance degradation due to the AWE. Figure 4 shows the effect of the number of antennas on the BER performance which presents the same tendency as in Fig. 3. From a practical point of view, there may be a physical restriction on increasing the number of antennas.

From now on, the effect of the AWE in the uplink synchronous DS-CDMA systems is investigated. The performance of the PIC receiver in the uplink synchronous system is evaluated and compared with that in the conventional uplink asynchronous system in terms of the various parameters such as the variance of the AWE and the number of antennas. Figure 5 shows that the uplink synchronous transmission in the PIC receiver may reduce the sensitivity to the AWE. For example, at the BER of 10^{-3} , the synchronous transmission may relax the tolerable variance of the AWE from 0.5 to 0.7 when $M=8$. This is because the orthogonality due to the uplink synchronous transmission makes the input signals at the first stage of the PIC more reliable. Additionally, we can see that the performance in the PIC receiver with the uplink synchronous transmission for $M=2$ is the same as that with the asynchronous transmission for $M=4$ when the variance of the AWE is 1. This means that a synchronous transmission with a smaller number of antennas can have the same performance as an asynchronous transmission with a larger number of antennas, when the AWE is large. In Fig. 6, at the BER of 10^{-3} , the number of users is shown as a function of the variance of the AWE in both uplink asynchronous and synchronous DS-CDMA systems when $E_b/N_0=20$ dB. When the variance of the AWE is 0.5, the capacity improvement in the PIC receiver in the uplink asynchronous DS-CDMA for $M=4$ is around 50% in

comparison with the case for $M=2$. Furthermore, when the variance of the AWE is 0.5, the improvement in the synchronous DS-CDMA PIC receiver for $M=4$ becomes 60% in terms of the number of users, when compared with the asynchronous DS-CDMA PIC receiver. In summary, the PIC receiver may achieve the capacity improvements by employing the uplink synchronous transmission as well as the larger number of antennas, even though the PIC receiver is very sensitive to the AWE. Tables 1 and 2 tabulate the user capacity in terms of the variance of the AWE and the number of antennas. Comparing Tables 1 and 2, we can see the break even points around 0.6 of the variance of the AWE for $M=8$, where the PIC cannot improve the performance further. Intuitively, we guess the effect of the AWE on the serial IC (SIC) receiver may be similar to that on the PIC receiver in this paper because both IC receivers will show a similar performance when perfect power control is assumed. If the power control is assumed to be imperfect, then the performance difference

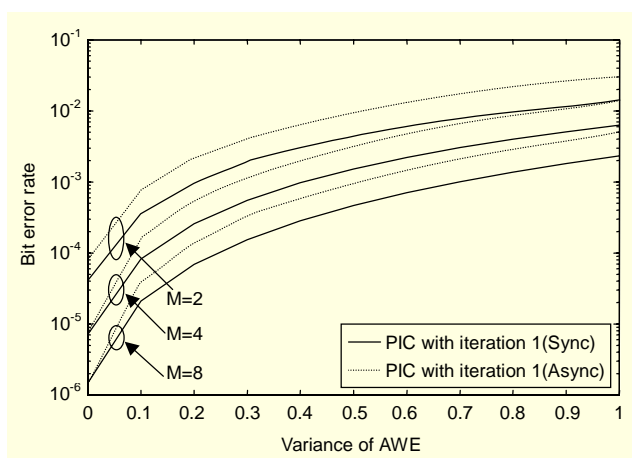


Fig. 5. BER vs. variance of the AWE in both asynchronous and synchronous DS-CDMA uplink ($K=72$, $E_b/N_0=20$ (dB)).

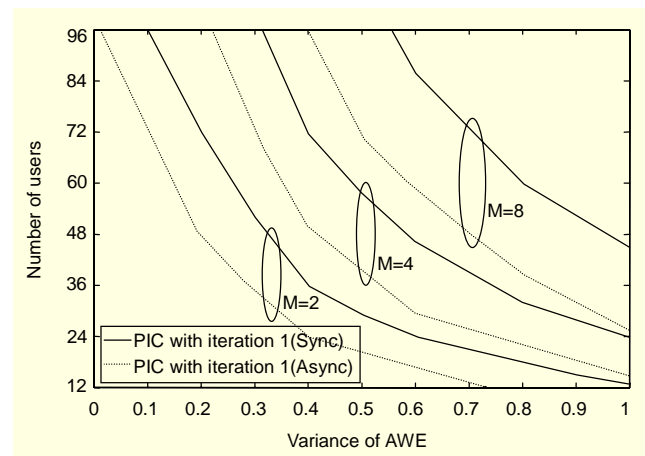


Fig. 6. Number of users vs. variance of the AWE in both async and sync DS-CDMA uplink ($E_b/N_0 = 20$ (dB), $BER=10^{-3}$).

Table 1. User capacity ($E_b/N_0 = 20$ (dB), $BER=10^{-3}$, PIC with iteration 1).

| Variance of the array weight error | User capacity ($BER=10^{-3}$) | | | | | |
|------------------------------------|---------------------------------|------|------|------|------|------|
| | Async | | | Sync | | |
| | M=2 | M=4 | M=8 | M=2 | M=4 | M=8 |
| 0.0 | > 96 | > 96 | > 96 | > 96 | > 96 | > 96 |
| 0.2 | 48 | > 96 | > 96 | 72 | > 96 | > 96 |
| 0.4 | 24 | 50 | 96 | 36 | 72 | > 96 |
| 0.6 | 16 | 30 | 58 | 24 | 46 | 86 |
| 0.8 | < 12 | 22 | 39 | 18 | 32 | 60 |
| 1.0 | < 12 | 15 | 26 | 13 | 24 | 45 |

Table 2. User capacity ($E_b/N_0=20$ (dB), BER= 10^{-3} , PIC with iteration 0).

| Variance of the array weight error | User capacity (BER= 10^{-3}) | | | | | |
|------------------------------------|---------------------------------|-----|------|------|-----|------|
| | Async | | | Sync | | |
| | M=2 | M=4 | M=8 | M=2 | M=4 | M=8 |
| 0.0 | 19 | 60 | > 96 | 29 | 96 | > 96 |
| 0.2 | 14 | 43 | > 96 | 23 | 70 | > 96 |
| 0.4 | < 12 | 31 | 77 | 18 | 48 | > 96 |
| 0.6 | < 12 | 24 | 59 | 14 | 36 | 90 |
| 0.8 | < 12 | 19 | 47 | < 12 | 30 | 72 |
| 1.0 | < 12 | 17 | 36 | < 12 | 25 | 60 |

between the SIC and the PIC would be seen. However, the difference may be decreased when the uplink synchronous transmission is employed.

V. Conclusions

In this paper, the effect of AWE in the PIC receiver in the uplink synchronous and asynchronous DS-CDMA system was investigated, when the AWE was modeled by be Gaussian distributed random variable. The performance degradation due to the AWE was estimated as a function of the variance of the AWE. Numerical results show that the performance of the PIC receiver with one iteration in the DS-CDMA uplink is more sensitive to the AWE than that of the RAKE receiver. However, either a larger number of antennas or uplink synchronous transmissions have the potential of reducing the overall sensitivity, and thus improving its performance. The consideration of more realistic assumptions such as the effect of power control [7], [23] and mutual coupling [24] is the subject of our future research. Additionally, more careful consideration of the SIC related with this work is also interesting for further study.

Appendix. Characteristics of Spatial Correlation Statistics

The spatial correlation can be expressed as

$$C_{lh}^{(k,m)} = \overline{\mathbf{W}_l^{(k)H}} \cdot \mathbf{V}(\theta_h^{(m)}) = \mathbf{V}^H(\theta_l^{(k)})\mathbf{V}(\theta_h^{(m)}) + \boldsymbol{\varepsilon}_l^{(k)H} \mathbf{V}(\theta_h^{(m)}).$$

The second order characterization of the spatial correlation is calculated as

$$E\left[\left\{C_{lh}^{(k,m)}\right\}^2\right] = E\left[\left\{\mathbf{V}^H(\theta_l^{(k)})\mathbf{V}(\theta_h^{(m)})\right\}^2\right] + E\left[\left\{\boldsymbol{\varepsilon}_l^{(k)H} \mathbf{V}(\theta_h^{(m)})\right\}^2\right],$$

where

$$\begin{aligned} & \left\{\mathbf{V}^H(\theta_l^{(k)})\mathbf{V}(\theta_h^{(m)})\right\}^2 \\ &= \sum_{i=0}^{M-1} (i+1) \exp(j2\pi di \cos\theta_l^{(k)}/\lambda) \cdot \exp(-j2\pi di \cos\theta_h^{(m)}/\lambda) \\ & \quad + \sum_{i=M}^{2(M-1)} (2M-i-1) \exp(j2\pi di \cos\theta_l^{(k)}/\lambda) \\ & \quad \times \exp(-j2\pi di \cos\theta_h^{(m)}/\lambda), \\ & \left\{\boldsymbol{\varepsilon}_l^{(k)H} \mathbf{V}(\theta_h^{(m)})\right\}^2 \\ &= \left\{\boldsymbol{\varepsilon}_l^{(k)H}\right\}^2 \cdot \sum_{i=0}^{M-1} \exp(j2\pi di \cos\theta_h^{(m)}/\lambda) \\ & \quad \times \exp(-j2\pi di \cos\theta_h^{(m)}/\lambda). \end{aligned}$$

Assuming the mean angles of arrival $\theta_l^{(k)}$ and $\theta_h^{(m)}$ have uniform distribution in $[0, \pi)$,

$$\begin{aligned} & E\left[\left\{\mathbf{V}^H(\theta_l^{(k)})\mathbf{V}(\theta_h^{(m)})\right\}^2\right] \\ &= \int_0^\pi \int_0^\pi \left\{\mathbf{V}^H(\theta_l^{(k)})\mathbf{V}(\theta_h^{(m)})\right\}^2 d\theta_l^{(k)} d\theta_h^{(m)} \\ &= \begin{cases} \sum_{i=0}^{M-1} (i+1) J_0(2\pi di/\lambda) J_0(-2\pi di/\lambda) \\ \quad + \sum_{i=M}^{2(M-1)} (2M-i-1) J_0(2\pi di/\lambda) J_0(-2\pi di/\lambda), & \text{if } k \neq m \text{ or } l \neq h, \\ M^2, & \text{if } k = m \text{ and } l = h, \end{cases} \end{aligned}$$

$$E\left[\left\{\boldsymbol{\varepsilon}_l^{(k)H} \mathbf{V}(\theta_h^{(m)})\right\}^2\right] = M \cdot \sigma_\varepsilon^2, \text{ for all } k, m, l, \text{ and } h,$$

where $J_0(x)$ is the zero order Bessel function of the first kind. Therefore,

$$\begin{aligned} & E\left[\left\{C_{lh}^{(k,m)}\right\}^2\right] \\ &= \begin{cases} M\sigma_\varepsilon^2 + \sum_{i=0}^{M-1} (i+1) J_0(2\pi di/\lambda) J_0(-2\pi di/\lambda) \\ \quad + \sum_{i=M}^{2(M-1)} (2M-i-1) J_0(2\pi di/\lambda) J_0(-2\pi di/\lambda), & \text{if } k \neq m \text{ or } l \neq h, \\ M\sigma_\varepsilon^2 + M^2, & \text{if } k = m \text{ and } l = h. \end{cases} \end{aligned}$$

Similarly, we can obtain the second order statistic of the estimated error component, expressed as follows:

$$\Delta_{lh}^{(k,m)} = \overline{\mathbf{W}_l^{(k)H}} \cdot \boldsymbol{\varepsilon}_h^{(m)} = \mathbf{V}^H(\theta_l^{(k)}) \cdot \boldsymbol{\varepsilon}_h^{(m)} + \boldsymbol{\varepsilon}_l^{(k)H} \cdot \boldsymbol{\varepsilon}_h^{(m)},$$

$$E\left[\left\{\Delta_{lh}^{(k,m)}\right\}^2\right] = E\left[\left\{V^H(\theta_l^{(k)})\boldsymbol{\epsilon}_h^{(m)}\right\}^2\right] + E\left[\left\{\boldsymbol{\epsilon}_l^{(k)H}\boldsymbol{\epsilon}_k^{(m)}\right\}^2\right],$$

where $E\left[\left\{\boldsymbol{\epsilon}_l^{(k)H}\boldsymbol{\epsilon}_k^{(m)}\right\}^2\right] = M\sigma_\epsilon^4$ can be easily determined by using the AWE statistics. Therefore the variance of the estimated error component is presented as

$$E\left[\left\{\Delta_{lh}^{(k,m)}\right\}^2\right] = M(\sigma_\epsilon^2 + \sigma_\epsilon^4), \text{ for all } k, m, l, \text{ and } h.$$

References

- [1] N. Mohamed and J. Dunham, "A Low Complexity Combined Antenna Array and Interference Cancellation DS-CDMA Receiver in Multipath Fading Channels," *IEEE J. Select. Area Comm.*, vol. 20, no. 2, Feb. 2002, pp. 248-256.
- [2] L. Tao and K.B. Letaief, "Multiuser Interference Cancellation with a Two-Dimensional RAKE Receiver for DS/CDMA Communications," *Proc. IEEE VTC'00*, 2000, pp. 1110-1114.
- [3] W. Ye and A.M. Haimovich, "Performance of Cellular CDMA with Cell Site Antenna Arrays, Rayleigh Fading, and Power Control Error," *IEEE Trans. Comm.*, vol. 48, no. 7, July 2000, pp. 1151-1159.
- [4] V. Ghazi-Moghadam and M. Kaveh, "A CDMA Interference Canceling Receiver with an Adaptive Blind Array," *IEEE J. Select. Area Comm.*, vol. 16, no. 8, Oct. 1998, pp. 1542-1554.
- [5] L.C. Godara, B.R. Tomiuk, N.C. Beaulieu, and A.A. Abu-Dayya, "Application of Antenna Arrays to Mobile Communication, Part II: BEAM-Forming and Direction-of-Arrival Considerations," *Proc. IEEE*, vol. 85, no. 8, Aug. 1997, pp. 1195-1245.
- [6] E.K. Hong, S.H. Hwang, K.J. Kim, and K.C. Whang, "Synchronous Transmission Technique for the Reverse Link in DS-CDMA Terrestrial Mobile System," *IEEE Trans. Comm.* vol. 47, no. 11, Nov. 1999, pp. 1632-1635.
- [7] S.H. Hwang and D.K. Kim, "Performance of Reverse-Link Synchronous DS-CDMA System on a Frequency-Selective Multipath Fading Channel with Imperfect Power Control," *EURASIP J. App. Sig. Proc.*, vol. 2002, no. 8, Aug. 2002, pp. 797-806.
- [8] 3GPP, TR25.854, *Uplink Synchronous Transmission Scheme*, May 2001 (<ftp://ftp.3gpp.org/>).
- [9] IEEE 802.20 C802.20-03/29, *Smart Antenna and MC-SCDMA*, Apr. 2003.
- [10] L. Hanzo, L.-L. Yang, E.-L. Kuan, and K. Yen, *Single- and Multicarrier DS-CDMA*, John Wiley & IEEE Press, 2003.
- [11] W. Sun, S.H. Hwang, D.K. Kim, and K.C. Whang, "Performance of Parallel Interference Cancellation with Reverse-Link Synchronous Transmission Technique for DS-CDMA System in Multipath Fading Channel," *IEICE Trans. Comm.*, vol. E85-B, no. 8, Aug. 2002, pp. 1622-1626.
- [12] Y.S. Kim, S.H. Hwang, D.K. Cho, and K.C. Whang, "Performance of Antenna Arrays with Reverse-Link Synchronous Transmission Technique for DS-CDMA System in Multipath Fading Channels," *Springer-Verlag Heidelberg, Lecture Notes in Computer Science*, vol. 2402, 2002, pp. 21-32.
- [13] Rec. ITU-R TG8-1, *Guideline for Evaluation of Radio Transmission Technologies for IMT-2000*, Rec. M.1225, 1997.
- [14] D. Parsons, *The Mobile Radio Propagation Channels*, Addison-Wesley, 1992.
- [15] J.G. Proakis, *Digital Communications*, McGraw-Hill, New York, 1983.
- [16] G. Raleigh, S.N. Diggavi, A.F. Naguib, and A. Paulraj, "Characterization of Fast Fading Vector Channels for Multi-Antenna Communication Systems," *Proc. IEEE ACSSC'94*, 1994, pp. 853-857.
- [17] Y. Kim and W. Yoon, "Efficiently Combined Structure of Smart Antenna and Interference Canceller Using Symbol Reliability," *IEE Electronics Lett.*, vol. 36, no. 18, Aug. 2000, pp. 1583-1584.
- [18] Y. Dai, G. Xue, T. Le-Ngoc, and J. Weng, "Combined Adaptive Interference Cancellation with Antenna Array for CDMA Systems," *Proc. IEEE GLOBECOM'00*, 2000, pp. 143-146.
- [19] A.F. Naguib, *Adaptive Antennas for CDMA Wireless Networks*, PhD dissertation, Stanford Univ., Stanford, CA, 1996.
- [20] Y.C. Yoon, R. Kohno, and H. Imai, "A Spread Spectrum Multiple Access System with Cochannel Interference Cancellation for Multipath Fading Channels," *IEEE J. Select. Area Comm.*, vol. 11, no. 7, Sept. 1993, pp. 1067-1075.
- [21] M.B. Pursley and D.V. Sarvate, "Evaluation of Correlation Parameters For Periodic Sequences," *IEEE Trans. Inform. Theory*, vol. IT-23, no. 4, July 1977, pp. 508-513.
- [22] T. Eng and L.B. Milstein, "Coherent DS-CDMA Performance in Nakagami Multipath Fading," *IEEE Trans. Comm.*, vol. 43, no. 2/3/4, Feb./Mar./Apr., 1995, pp. 1134-1143.
- [23] J.G. Andrews and T.H. Meng, "Optimum Power Control for Successive Interference Cancellation with Imperfect Channel Estimation," *IEEE Trans. Wireless Comm.*, vol. 2, no. 2, Mar. 2003, pp. 375-383.
- [24] K.R. Dandekar, H. Ling, and G. Xu, "Effect of Mutual Coupling on Direction Finding in Smart Antenna Applications," *IEE Electronics Lett.*, vol. 36, no. 22, Oct. 2000, pp. 1889-1891.



Yong-Seok Kim was born in August 1970, in Seoul, Korea. He received the BS degree in electronic engineering from the Kyunghee University, Yongin-si, Korea, in 1998 and the MS degree in electrical and computer engineering from Yonsei University, Seoul, Korea in 2000, and is working toward the PhD degree in electrical and electronic engineering at the same university. His current research interests include multiple antenna system, multi-user communication, multi-carrier system and 4G communication techniques.



Seung-Hoon Hwang was born in Seoul, Korea on February 26, 1969. He received the BS, MS and PhD degrees in electrical engineering from Yonsei University, Seoul, Korea in 1992, 1994 and 1999, respectively. In March 1999, he joined the LG Electronics, Anyang, Korea, where he is a Chief Research Engineer in Communication & Mobile R&D Center, participating in UMTS physical layer standardization activities. From May 2003, he is currently a Visiting Research Fellow at the School of Electronics and Computer Science in University of Southampton, United Kingdom. His research interests include interference reduction techniques for wireless CDMA systems, various aspects of wideband/broadband CDMA, and wireless Multi-Carrier DS-SS-CDMA systems. Dr. Hwang is a Recipient of the British Chevening Scholarship awarded by the British council, U.K. in 2003 and the Postdoctoral Fellowship from the Korea Science and Engineering Foundation (KOSEF), Korea in 2004.



Keum-Chan Whang was born on July 18, 1944, in Seoul, Korea. He received the BS degree in electrical engineering from Yonsei University, Seoul, Korea, in 1967 and the MS and PhD degrees from the Polytechnic Institute of New York, in 1975 and 1979, respectively. From 1979 to 1980, he was a

Member of Research Staff at the Agency for Defense Development, Korea. Since 1980, he has been Professor of the Department of Electrical and Electronic Engineering, Yonsei University. For the government, he performed various duties such as being a Member of Radio Wave Application Committee, a Member of Korea Information & Communication Standardization Committee, and is an Advisor for the Ministry of Information and Communication's Technology Fund and a Director of Accreditation Board for Engineering Education of Korea. Currently, he serves as a Member of Korea Communications Commission, a Project Manager of Qualcomm-Yonsei Research Lab and a Director of Yonsei's IT Research Center. His research interests include spread-spectrum systems, multi-user communications, and 4G communications techniques.